Journal of Biomolecular NMR, **26:** 241–247, 2003.
KLUWER/ESCOM

Cross-correlation suppressed T_1 and NOE experiments for protein side-chain $^{13}CH_2$ groups

Changwen Jin[a], Jeanine J. Prompers[b] & Rafael Brüschweiler*
Carlson School of Chemistry and Biochemistry, Clark University, Worcester, MA 01610, U.S.A.
Present addresses: [a]*Beijing NMR Center, Peking University, Beijing, China;* [b]*Eindhoven University of Technology, Biomedical NMR, Eindhoven, The Netherlands*

Received 23 December 2002; Accepted 6 March 2003

Key words: methylene groups, NMR relaxation, NOE, protein side-chain dynamics, suppression of cross-correlated relaxation, T_1

Abstract

Relaxation measurements of side-chain $^{13}CH_2$-groups of uniformly ^{13}C labeled human ubiquitin were performed at 600 MHz and 800 MHz magnetic field strength at 30 °C. Dipole-dipole cross-correlated relaxation effects in T_1 experiments were suppressed by the combination of radio-frequency pulses and pulsed field gradients during the relaxation delay leading to monoexponential relaxation decays that allow a more accurate extraction of the ^{13}C T_1 relaxation times. Heteronuclear $\{^1H\}$-^{13}C NOEs obtained by using different proton saturation schemes indicate that the influence of cross-correlation is small. The experimental T_1 and NOE data were interpreted in a model-free way in terms of a generalized order parameter and an internal correlation time.

Introduction

The detailed characterization of protein dynamics is important for the understanding of protein function. Nuclear magnetic resonance (NMR) spin relaxation is a powerful method to provide dynamics information on pico- to nanosecond and micro- to millisecond time scales (Kay, 1998; Ishima and Torchia, 2000; Palmer, 2001). The majority of NMR relaxation studies of proteins focus on backbone ^{15}N relaxation and only relatively few studies investigate the side chains. Methyl groups are the most commonly used probes of side-chain dynamics (Nicholson et al., 1992; Muhandiram et al., 1995; Wand et al., 1996; Gagne et al.., 1998; Ishima et al., 1999; Lee et al., 2000; Millet et al., 2002; Skrynnikov et al., 2002).

Nearly 50% of the carbon atoms in amino-acid side chains belong to methylene moieties whose relaxation behavior provides unique dynamic information. Auto-relaxation studies of $^{13}CH_2$ groups face specific challenges: (i) The CH_2 groups are usually less mobile than methyl groups, which leads to larger line widths and therefore to lower sensitivity and a higher occurrence of spectral overlap. (ii) The $^{13}CH_2$ moiety is a three-spin 1/2 system, which exhibits dipole-dipole cross-correlated relaxation (Werbelow and Grant, 1977). Cross-correlated relaxation can cause multi-exponential relaxation affecting ^{13}C T_1 and NOE auto-relaxation parameters in a complex way (Zhu et al., 1995). Cross-correlation effects can be suppressed by partial deuteration in combination with selective ^{13}C labeling (LeMaster and Kushlan, 1996) or random fractional deuteration in uniformly ^{13}C-enriched samples (Yang and Kay, 1996). (iii) In fully ^{13}C-labeled samples dipolar relaxation between adjacent carbons can influence the measured ^{13}C auto-relaxation rates provided that the overall rotational tumbling is very slow. Yamazaki et al. (1994) studied the relaxation properties of $^{13}C^{\alpha}$ carbons in uniformly ^{13}C labeled alanine over a temperature range between 10 °C and 40 °C, corresponding to tumbling correlation times between 1 ns and 17 ns. It was found that at lower temperatures carbon-carbon dipole relaxation significantly affects C^{α} relaxation times,

*To whom correspondence should be addressed. E-mail: bruschweiler@nmr.clarku.edu

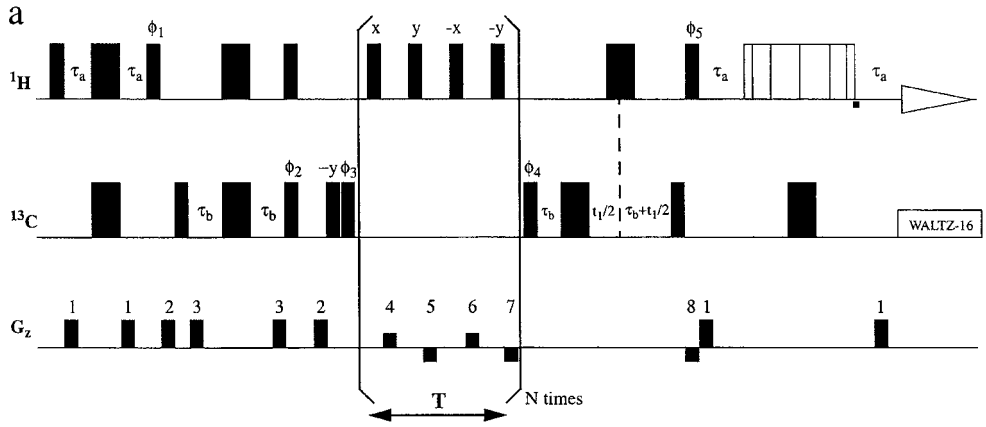

Figure 1. Pulse sequence for measuring (a) the ^{13}C T_1 relaxation times and (b) {^{1}H}-^{13}C NOEs of CH_2 groups in uniformly ^{13}C labeled protein samples. In Panel b, the region in the sequence marked with B is to be replaced by the elements B1, B2, or B3 given at the bottom. Narrow and wide bars correspond to pulses with a flip angle of 90° and 180° pulses, respectively. The pulses are applied along the x axis unless indicated otherwise. All proton pulses had a 32 kHz field strength, which corresponds to a 90° pulse length of 7.8 μs, except for saturation and WALTZ-16 decoupling pulses, which had a field strength of 8.9 kHz and 5.6 kHz, respectively. All carbon pulses (centered at 43 ppm) were applied with a 20 kHz field strength and WALTZ-16 was employed for decoupling during the acquisition period with a field strength of 2.6 kHz. In the NOE experiment of panel b during the constant-time period $^{13}C'$ carbonyl decoupling is applied as indicated by dashed vertical lines and ^{15}N decoupling is employed by using WALTZ-16 with 1 kHz field strength centered at 119 ppm. In panel a, the 90°_{-y} $90^\circ_{\phi 3}$ pulse pair preceding the relaxation period is optional. Water suppression is obtained using WATERGATE implemented with a 3-9-19-19-9-3 pulse (Sklenar et al., 1993). The delays used are as follows: $\tau_a = 1.7$ ms, $\tau_b = 0.85$ ms, $\delta = 13.3$ ms. The following phase cycles were used. (a) $\phi_1 = 8(y), 8(-y)$; $\phi_2 = y, y, -y, -y$; $\phi_3 = y, -y$; $\phi_4 = 4(-y), 4(y)$; $\phi_5 = -x$; rec = y, −y, −y, y, −y, y, y, −y, −y, y, y, −y, y, −y, −y, y. (b) $\phi_1 = 16(x), 16(-x)$; $\phi_2 = x, y, -x, -y$; $\phi_3 = 4(y), 4(-y)$; $\phi_4 = 8(x), 8(-x)$; rec = 2(x, −x), 2(−x, x), 2(x, −x), 2(−x, x), 2(−x, x), 2(x,−x), 2(−x, x), 2(x, −x). The gradients used in (a) are g1 = (0.9 ms, 4 G cm^{-1}), g2 = (2 ms, 4.4 G cm^{-1}), g3 = (0.5 ms, 8.3 G cm^{-1}), g4 = (0.3 ms, 0.7 G cm^{-1}), g5 = (0.3 ms, −1.4 G cm^{-1}), g6 = (0.3 ms, 1.4 G cm^{-1}), g7 = (0.3 ms, −0.7 G cm^{-1}), g8 = (1.2 ms, −2.6 G cm^{-1}), while for sequence in (b) g1 = (0.5 ms, 6.5 G cm^{-1}), g2 = (0.5 ms, 22 G cm^{-1}), g3 = (0.4 ms, 4.4 G cm^{-1}). Quadrature detection along t_1 was achieved by States-TPPI.

while at higher temperatures and thus shorter tumbling correlation times such effects are small.

In this work modified T_1 and NOE relaxation experiments are described that suppress dipole-dipole cross-correlated relaxation. The experiments are used for relaxation measurements of side-chain CH_2 groups of uniformly ^{13}C labeled human ubiquitin at two magnetic fields.

Materials and methods

NMR sample

A sample of uniformly ^{15}N, ^{13}C labeled human ubiquitin was obtained from VLI-research (Southeastern, PA). The sample contained about 4 mM ubiquitin in 50% D_2O/ 50% H_2O with a 45 mM sodium acetate buffer at pH 4.7. The sample was deoxygenated and sealed in a standard 5 mm NMR sample tube.

NMR pulse sequences

The 2D NMR pulse scheme for measuring T_1 parameters of CH_2 groups is shown in Figure 1a. It consists of the following steps. Magnetization is first transferred from ^{1}H to ^{13}C spins via a refocused INEPT, $H_z \rightarrow C_z$. During the following relaxation delay, C_z undergoes longitudinal relaxation. At the same time the three-spin order term $C_z H_{1z} H_{2z}$ is created due to ^{13}C-^{1}H,^{13}C-^{1}H dipole-dipole cross-correlated relaxation. These unwanted spin terms are purged as follows. A 90° proton pulse is applied first, which generates double- and zero-quantum coherence of the type $C_z H_1^+ H_2^+$, $C_z H_1^- H_2^-$, and $C_z H_1^+ H_2^-$, $C_z H_1^- H_2^+$, respectively. The double-quantum terms are destroyed by the application of a pulsed field gradient (PFG), while the zero-quantum terms are partially converted into double-quantum terms by additional 90° proton pulses with different phases. These double-quantum terms are subsequently destroyed by PFGs as is indicated in Figure 1a. The N-fold repetition of this procedure counteracts the relaxation-induced production of three-spin order terms during the delay $N \cdot T$

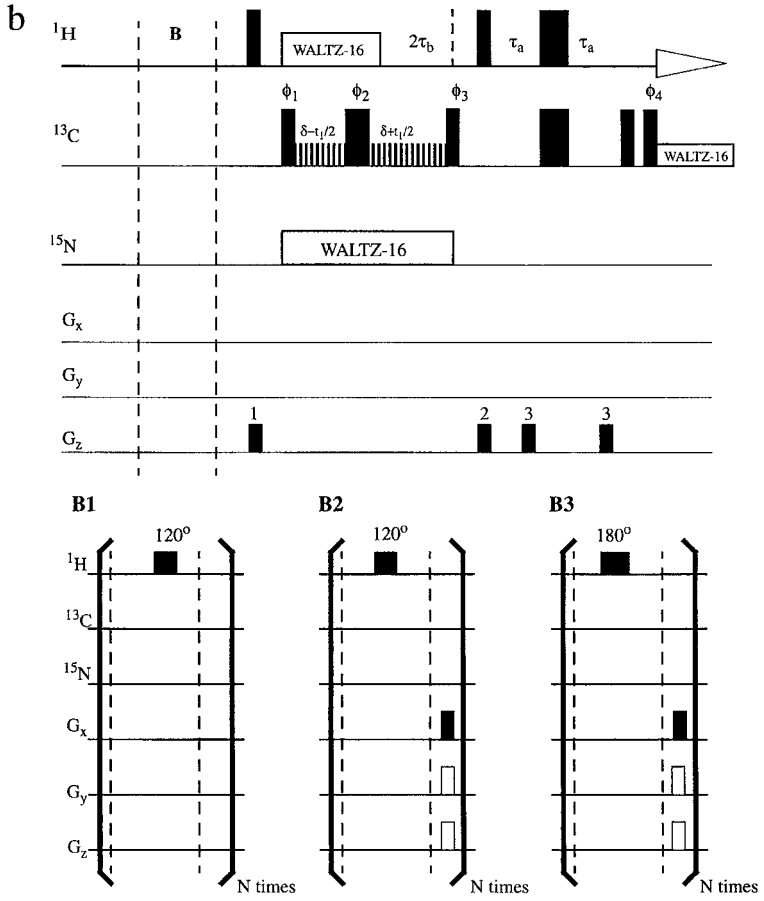

Figure 1. Continued.

where N is an integer number. During the t_1 period magnetization of ^{13}C nuclei undergoes precession under the chemical shift Hamiltonian and is then back-transferred to the directly coupled protons for detection during t_2.

To assess the performance of the suppression scheme, two control experiments were performed. In the first experiment, 90° proton pulses without PFGs were applied during the delay and in the second one 180° proton pulses were applied together with PFGs. The effects of dipole-CSA cross-correlated relaxation rates, which are small due to the small size of ^{13}C CSA tensors in methylene groups, were eliminated by the proton pulses applied during the delay $N \cdot T$ of Figure 1a (Boyd et al., 1990).

T_1 relaxation times were determined from exponential fitting of the cross-peak intensities of a series of 2D spectra collected with different relaxation delays $N \cdot T$ using the pulse sequence of Figure 1a. A fit to the function $I(N \cdot T) = a_0 \exp(-N \cdot T / T_1)$ was performed for each cross-peak intensity series $I(N \cdot T)$ with a_0 and T_1 as fit parameters using the program NMRView (B. Johnson, Merck and Co., Inc.).

The pulse sequence for measuring the $\{^1$H$\}$-^{13}C NOE values of CH_2 groups is given in Figure 1b. It is based on the sequence of Yamazaki et al. (1994) for the measurement of main chain $^{13}C^{\alpha}$ T_1 relaxation. Proton saturation is achieved by applying a series of 120° pulses (Markley et al., 1971) with or without PFGs (elements B1 and B2 of Figure 1b) or by a series of 180° pulses with PFGs (element B3). The original magnetization originates from equilibrium magnetization of ^{13}C nuclei. ^{1}H decoupling is applied immediately after the excitation of carbon magnetization and stopped at the time $2\tau_b = 1/(4\ ^1J_{HC})$ prior to the INEPT transfer of the carbon magnetization to the directly attached protons. The constant-time chemical shift evolution period was set to $2\delta = 1/^1J_{CC}$ to obtain adequate resolution in the 2D ^{13}C-^{1}H correlation spectra along the ^{13}C dimension,

Table 1. Experimental vs. back-calculated relaxation parameters

Relation parameter	600 MHz		800 MHz	
	$\frac{T_1^{exp}-T_1^{calc}}{T_1^{exp}}$	$\frac{NOE^{exp}-NOE^{calc}}{NOE^{exp}}$	$\frac{T_1^{exp}-T_1^{calc}}{T_1^{exp}}$	$\frac{NOE^{exp}-NOE^{calc}}{NOE^{exp}}$
Error (%)	10.7	3.0	6.7	2.2

where $^1J_{CC}$ is the aliphatic carbon-carbon coupling constant (Santoro and King, 1992; Vuister and Bax, 1992). To assess the effect of cross-correlated relaxation, different experiments were performed with the pulse-sequence elements B1, B2, or B3. The heteronuclear NOE values were determined using the ^{13}C-^{1}H cross-peak intensities obtained with and without saturation of the protons using the heteronuclear NOE analysis module of NMRView.

Results and discussion

Relaxation measurements

The longitudinal spin dynamics of a $^{13}CH_2$-moiety in the absence of radio-frequency (rf) pulses is governed in good approximation by the Master equation (Werbelow and Grant, 1977)

$$\frac{d\boldsymbol{m}}{dt} = R\{\boldsymbol{m}(t) - \boldsymbol{m}_{eq}\}. \quad (1)$$

With one-spin polarization, C_z, as initial condition and if dipole-CSA cross-correlated relaxation can be neglected, $\boldsymbol{m}$ is a four-dimensional column vector consisting of the expectation values of one- and three-spin order terms $m = (\langle C_z\rangle, \langle H_{1z}\rangle, \langle H_{2z}\rangle, \langle 4C_zH_{1z}H_{2z}\rangle)$; $\boldsymbol{m}_{eq}$ contains the corresponding expectation values at thermal equilibrium. The diagonal elements of the 4 × 4 rate matrix $\boldsymbol{R}$ are the auto-relaxation rate constants of the individual spin terms and the off-diagonal elements are the auto- and cross-correlated (cross-relaxation) rate constants between the different spin terms. Since the solution of Equation 1 is multi-exponential, the accurate determination of individual elements of $\boldsymbol{R}$ is not straightforward. The relaxation behavior can be simplified by the application of rf pulses and PFGs during the relaxation period $N \cdot T$ of Figure 1a: The goal is the accurate determination of element $R_{11} = 1/T_1(C)$ by 'decoupling' the evolution of magnetization C_z from all other terms. While decoupling of C_z from H_{1z} and H_{2z} is accomplished by irradiation of the protons, the dipole-dipole cross-correlation process $C_z \rightarrow 4C_zH_{1z}H_{2z}$ cannot be suppressed by (non-selective) proton pulses only. Therefore, the suppression scheme shown in Figure 1a uses a combination of 90° proton pulses and PFGs as described above. In contrast, 180° proton pulses would not have the desired effect because they leave the $4C_zH_{1z}H_{2z}$ term invariant.

The performance of the pulse sequence of Figure 1a is shown in Figure 2 for selected $^{13}CH_2$ groups at 600 and 800 MHz (Figures 2a, c and 2d). The relaxation decays follow in very good approximation monoexponential behavior. In contrast, if during delay T the 90° pulses are replaced by 180° pulses, the dipole-dipole cross-correlated evolution $C_z \rightarrow 4C_zH_{1z}H_{2z}$ occurs uninhibited and can lead to a pronounced multi-exponential decay behavior as is illustrated in Figure 2b. Analogously, if during delay T the 90° proton pulses are retained but the PFGs are removed, multi-exponential decay is observed (not shown). Multi-exponential relaxation behavior due to dipolar ^{13}C-^{13}C relaxation is not manifested, since for the relatively short overall tumbling correlation time of ubiquitin (< 5 ns) such relaxation effects are small (Yamazaki, 1994).

Heteronuclear NOEs were measured using the pulse sequence of Figure 1b with three different saturation schemes B1, B2, and B3. The NOE differences among the different saturation schemes are comparable to the experimental errors, which indicates that cross-correlated relaxation effects have only a minor influence on the heteronuclear NOE. T_1 and NOE data of good quality at 600 and 800 MHz proton frequency could be obtained for non-overlapping cross peaks for 30 $^{13}CH_2$ side-chain groups and the backbone $^{13}C^{\alpha}H_2$ of Gly 10. The data are displayed in Figure 3. For CH_2 groups for which the intensities of both C-H cross peaks could be measured, the relaxation parameters were analyzed separately for each cross peak and then averaged.

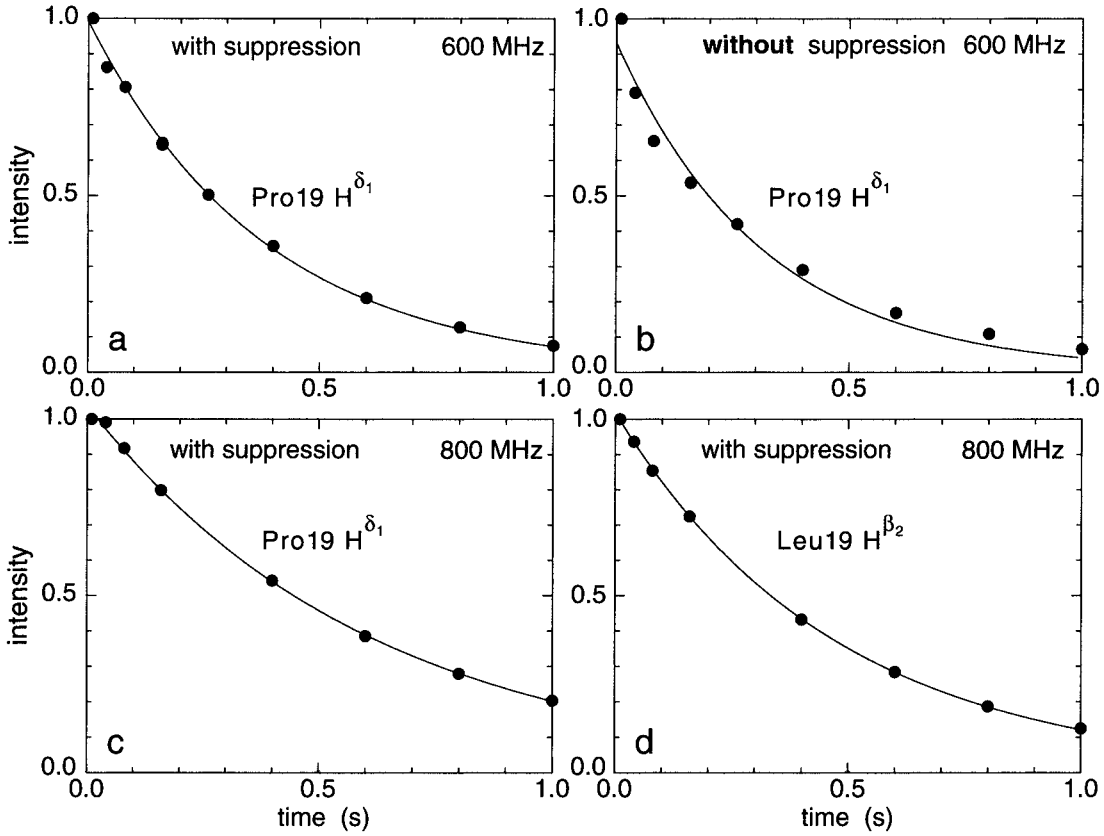

Figure 2. Experimental T_1 relaxation curves of the $^{13}CH_2$ groups of C^{δ} of Pro 19 (a, b, c) and C^{β} of Leu 43 (d) of uniformly ^{15}N and ^{13}C labeled ubiquitin at two B_0 magnetic fields using the pulse sequence of Figure 1a. Decay curves of the C-H cross-peak intensities in (a), (c), (d) were obtained using suppression of cross-correlated relaxation, while the decay curve of (b) was obtained by replacing the 90° pulses during the relaxation delay T (Figure 1a) by 180° pulses rendering the suppression ineffective.

Model-free analysis

The relaxation parameters were analyzed on a residue-by-residue basis using the model-free approach by Lipari and Szabo (1982). Two local model-free parameters, the generalized order parameter S^2 and the internal correlation time τ_{int}, were fitted together with an overall tumbling correlation time τ_c. Because conformational exchange processes do not affect the T_1 and NOE data, the model-free analysis is rather straightforward. It was applied separately to the T_1 and NOE relaxation data at 600 MHz and at 800 MHz as well as to the combined data at both fields. The overall tumbling correlation time was set to $\tau_c = 4.75$ ns, which was determined from backbone ^{15}N relaxation experiments. The results are shown in Figure 4. The error bars were determined using a Monte Carlo error analysis with 100 runs. The three analyses give for most CH_2 groups consistent results for the order parameters with S^2 differences below 0.12 indicating that a two-parameter model works quite well for these residues. Exceptions are C^{β} of Ser 20, C^{γ} of Pro 36, and C^{β} of Leu 56 for which the S^2 parameter extracted at 600 MHz is highest and the one at 800 MHz is lowest. For those methylene groups for which all relaxation parameters could be determined for both cross peaks, the individual order parameters generally differ by less than 2%.

Most internal correlation times τ_{int} are below 500 ps. Their relative uncertainties are on average larger than the ones of the S^2 values. For very high S^2 values, such as the ones found for C^{β} of Lys 27 and C^{γ} of Gln 41, the τ_{int} values are notably underdetermined. The relaxation parameters were back-calculated from the best fitting model-free parameters and compared with the experimental relaxation data. The average differences, which are given in Table 1, vary between 2% and 11% for the combined fitting of the data at 600 and 800 MHz. With the exceptions mentioned

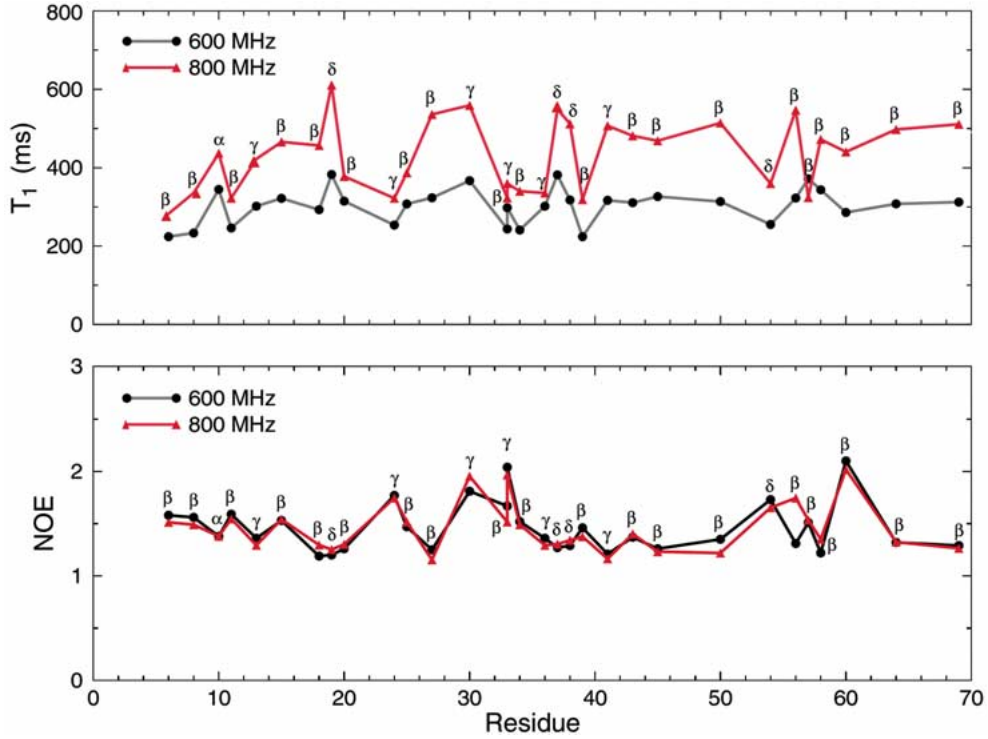

Figure 3. Experimental T_1 and NOE relaxation parameters of $^{13}CH_2$ groups of uniformly ^{13}C labeled ubiquitin at 600 MHz (black) and 800 MHz (red) proton frequency using the pulse sequences of Figure 1.

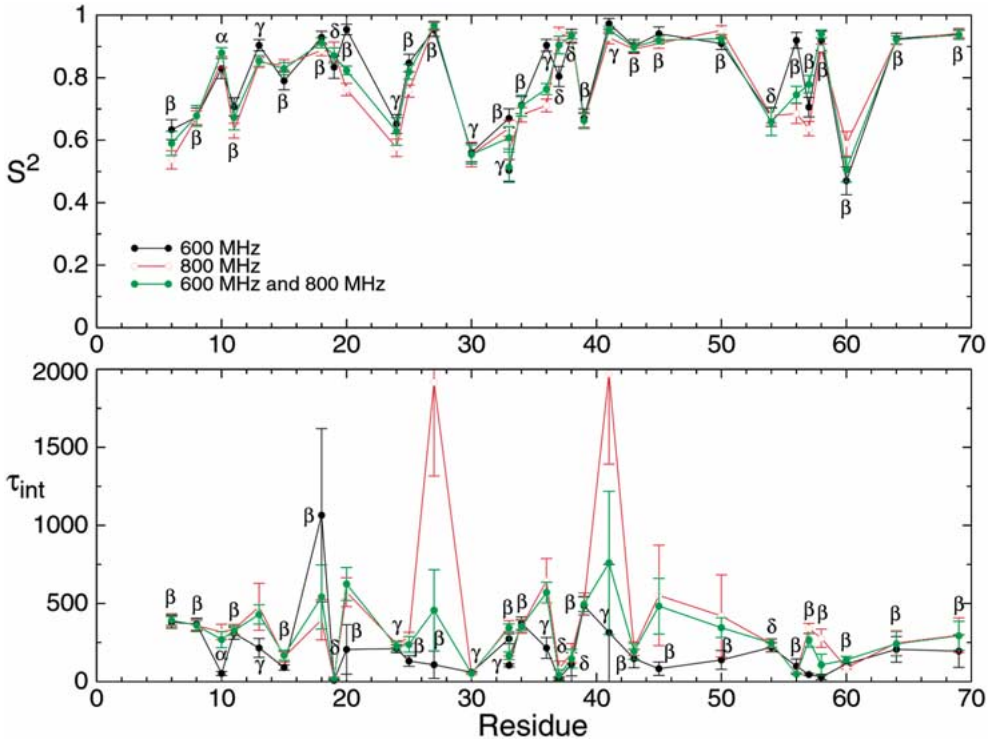

Figure 4. Model-free analysis of the $^{13}CH_2$ relaxation parameters of Figure 3 in terms of a S^2 order parameter and an internal correlation time τ_{int}. Model-free parameters were obtained by separately fitting T_1 and NOE data at 600 MHz (black) and at 800 MHz (red), and by combined fitting of T_1 and NOE data at both field strengths (green). The error bars were obtained by Monte Carlo simulations.

above, the relaxation behavior of most CH_2 groups is well captured by the model-free analysis with internal correlation times falling into the subnanosecond time-scale range. The generalized S^2 order parameters vary between 0.5 and 0.95 reflecting a larger variability than what is found for the corresponding N-H backbone order parameters (Wand et al., 1992; Tjandra et al., 1995; Lienin et al., 1998). No significant correlations between side-chain and backbone order parameters or between side-chain order parameters and secondary structure and amino-acid type could be detected.

In summary, the 2D NMR relaxation experiments presented here allow the quantitative measurement of longitudinal relaxation times and heteronuclear NOEs of $^{13}CH_2$ groups in biomolecules by suppressing dipole-dipole cross-correlated relaxation induced three-spin order. The relaxation data of ubiquitin collected at 600 and 800 MHz magnetic field strength could in most cases consistently be described in a model-free way. For small to medium large proteins, the pulse sequences can be applied to uniformly ^{13}C-labeled samples, such as the ones typically used for protein structure determination, overcoming the need of partial or specific deuteration.

Acknowledgements

We thank Dr Mark Rance for kindly providing NMR time on the 800 MHz spectrometer at the University of Cincinnati. This work was supported by NSF Grant No. MCB-0211512.

References

Boyd, J., Hommel, U. and Campbell, I.D. (1990) *Chem. Phys. Lett.*, **175**, 477.

Gagne, S.M., Tsuda, S., Spyracopoulos, L., Kay, L.E. and Sykes, B.D. (1998) *J. Mol. Biol.*, **278**, 667–686.

Ishima, R. and Torchia D.A. (2000) *Nat. Struct. Biol. NMR*, **7**, 740–743.

Ishima, R., Louis, J.M. and Torchia, D.A. (1999) *J. Am. Chem. Soc.*, **121**, 11589–11590.

Kay, L.E. (1998) *Nat. Struct. Biol. NMR*, **5** (Suppl.), 513–516.

Lee, A.L., Kinnear, S.A. and Wand, A.J. (2000) *Nat. Struct. Biol.*, **7**, 72–77.

LeMaster, D.M. and Kushlan, D.M. (1996) *J. Am. Chem. Soc.*, **118**, 9255–9264.

Lienin, S.F., Bremi, T., Brutscher, B., Brüschweiler, R. and Ernst, R.R. (1998) *J. Am. Chem. Soc.*, **120**, 9870–9879.

Lipari, G. and Szabo, A. (1982) *J. Am. Chem. Soc.*, **104**, 4546–4559.

Markley, J.L., Horsley, W.J. and Klein, M.P. (1971) *J. Chem. Phys.*, **55**, 3604–3605.

Millet, O., Muhandiram, D.R., Skrynnikov, N.R. and Kay, L.E. (2002) *J. Am. Chem. Soc.*, **124**, 6439–6448.

Muhandiram, D.R., Yamazaki, T., Sykes, B.D. and Kay, L.E. (1995) *J. Am. Chem. Soc.*, **117**, 11536–11544.

Nicholson, L.K., Kay, L.E., Baldisseri, D.M., Arango, J., Young, P.E., Bax, A. and Torchia, D.A. (1992) *Biochemistry*, **31**, 5253–5263.

Palmer, A.G. (2001) *Annu. Rev. Biophys. Biomol. Struct.*, **30**, 129–155.

Santoro, J. and King, G.C. (1992) *J. Magn. Reson.*, **97**, 202–207.

Schneider, D.M., Dellwo, M.J. and Wand A.J. (1992) *Biochemistry*, **31**, 3645–3652.

Sklenar, V., Piotto, M., Leppik, R. and Saudek, V. (1993) *J. Magn. Reson. A*, **102**, 241–245.

Skrynnikov, N.R., Millet, O. and Kay, L.E. (2002) *J. Am. Chem. Soc.*, **124**, 6449–6460.

Tjandra, N., Feller, S.E., Pastor, R.W. and Bax A. (1995) *J. Am. Chem. Soc.*, **117**, 12562–12566.

Vuister, G.W. and Bax, A. (1992) *J. Magn. Reson.*, **98**, 428–435.

Wand, A.J., Urbauer, J.L., McEvoy, R.P. and Bieber, R.J. (1996) *Biochemistry*, **35**, 6116–6125.

Werblow L.G. and Grant D.M. (1977) *Adv. Magn. Reson.*, **9**, 189–299.

Yamazaki, T., Muhandiram, R. and Kay, L.E. (1994) *J. Am. Chem. Soc.*, **116**, 8266–8278.

Yang, D. and Kay, L.E. (1996) *J. Magn. Reson. B*, **110**, 213–218.

Zhu, L., Kemple, M.D., Landy, S.B. and Buckley, P. (1995) *J. Magn. Reson. B*, **109**, 19–30.